

Dielectric droplet on a superhydrophobic substrate in an electric field

A. L. Kupershtokh

National Research Novosibirsk State University
Novosibirsk, Russia
skn@hydro.nsc.ru

D.A. Medvedev

Lavrentyev Institute of Hydrodynamics of SB RAS
Novosibirsk, Russia
dmedv@hydro.nsc.ru

Abstract—A non-stationary electrohydrodynamic model of a dielectric droplet dynamics on solid substrate in surrounding gas is developed. The equations for electric field potential and fluid dynamics are solved together. Computer 3D simulations of liquid dielectric droplets on wettable and superhydrophobic surfaces are carried out. The dynamics of the pinned droplet is also simulated. The droplets tend to elongate in the direction of DC electric field. The droplet can jump over a superhydrophobic substrate after the electric field is applied.

Keywords—droplet, dielectric liquid, electric field, computer simulations, graphics processing unit, superhydrophobic substrate

I. INTRODUCTION

The understanding of the behavior of droplets placed on the superhydrophobic substrates is very important for modern technologies. The electric field affects the behavior of liquid droplets. It can enhance the heat transfer from the solid substrate [1] and can also be used to manipulate droplets [2]. Many studies, experimental [1,3-6], theoretical [4-7], and with computer simulations [8-10] are devoted to investigation of the behavior of droplets and bubbles under the action of an electric field. The equilibrium shape of a droplet (both dielectric and conductive) is determined by the surface tension, as well as by electrical and gravity forces.

However, the computer simulations of non-stationary growth and deformation of droplets in electric field are practically absent. This is mainly due to the complexity of computer simulation of two-phase gas-liquid systems, taking into account surface tension, gravity and electrical forces. Recently, a new method of computer modeling of such processes has appeared. This lattice Boltzmann method (LBM) [11-13] is a powerful tool for modeling such complex multiphysical phenomena.

In the present work, three-dimensional computer simulations of a dynamics of a liquid dielectric droplet that placed onto a horizontal substrate in DC electric field is carried out. Spherical or hemispherical liquid dielectric droplets are placed onto a superhydrophobic or wettable horizontal substrate. The substrate is electrically grounded. High voltage is applied to the upper flat electrode.

The electrical and hydrodynamic parts of the problem are solved simultaneously. The lattice Boltzmann method is used for simulations of this nonstationary problem of droplet dynamics. This method allows one to take into account the surface tension on the liquid-vapor interface, the external forces (electrostatic and gravity forces) and also the interaction of fluid with solid substrate. The distribution of the electric field strength in the entire region between the flat electrodes is calculated numerically at each time step by solving the Poisson's equation for the potential of the electric

field. The spatial distribution of the dielectric permittivity of the liquid varies in the process of simulations. The CUDA (Compute Unified Device Architecture) technology is used for parallel programming on the "Supermicro 4027GR" computer that consists of several graphics processing units (GPUs). Parallel calculations are performed simultaneously using all cores of GPUs (GTX Titan-Xp).

II. LATTICE BOLTZMANN EQUATION METHOD

Lattice Boltzmann method considers the fluid flows as an ensemble of pseudoparticles that can move along the links of the 3D lattice. The velocities of pseudoparticles take the limited set of values $|\mathbf{c}_k| = 0, h/\Delta t$ and $\sqrt{2}h/\Delta t$ (Fig. 1) [14]. The evolution equations for distribution functions N_k have the form

$$N_k(\mathbf{x} + \mathbf{c}_k \Delta t, t + \Delta t) = N_k(\mathbf{x}, t) + \Omega_k \{N_k(\mathbf{x}, t)\} + \Delta N_k. \quad (1)$$

Here, the collision operator has the BGK form [14]

$$\Omega_k(N_k(\mathbf{x}, t)) = \frac{N_k^{eq}(\rho, \mathbf{u}) - N_k(\mathbf{x}, t)}{\tau}. \quad (2)$$

The dimensionless relaxation time τ determines the kinematic viscosity of fluid $\nu = (\tau - 1/2)\theta\Delta t$. Equilibrium distribution functions N_k^{eq} are usually taken in the form [15]

$$N_k^{eq}(\rho, \mathbf{u}) = \rho w_k \left(1 + \frac{(\mathbf{c}_k \cdot \mathbf{u})}{\theta} + \frac{(\mathbf{c}_k \cdot \mathbf{u})^2}{2\theta^2} - \frac{\mathbf{u}^2}{2\theta} \right). \quad (3)$$

The density ρ and the velocity of fluid \mathbf{u} are calculated as the first and the second moments of the distribution functions N_k .

We use the Exact Difference Method (EDM) [16,17] for the change of distribution functions ΔN_k due to the body

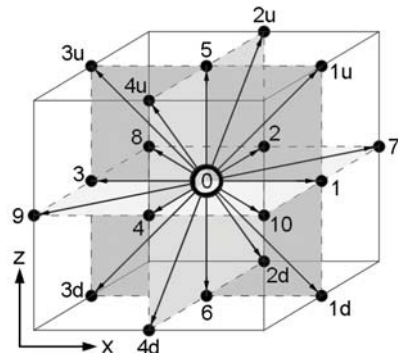


Fig. 1. Set of the possible velocity vectors \mathbf{c}_k for the nineteen-speed LB model D3Q19.

The study was supported by the Russian Science Foundation (Grant No. 18-19-00538).

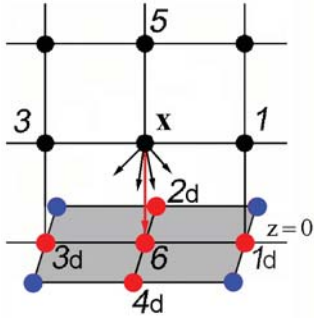


Fig. 2. Interaction forces between a fluid node \mathbf{x} and the nearest five nodes at solid substrate (red points).

forces (internal and external)

$$\Delta N_k = N_k^{eq}(\rho, \mathbf{u} + \Delta \mathbf{u}) - N_k^{eq}(\rho, \mathbf{u}). \quad (4)$$

Here, the change in velocity during the time step is equal to $\Delta \mathbf{u} = \mathbf{F} \Delta t / \rho$. The internal forces between nodes were introduced to simulate the phase transition. These forces are expressed as the gradient of the pseudopotential $\mathbf{F}_{\text{int}}(\mathbf{x}) = -\nabla U$, where $U = P(\rho, T) - \rho \theta$ [18]. We proposed earlier to use a special function $\Phi = \sqrt{-U}$. Then, the formula for the internal forces can be rewritten in the equivalent form [19,20]

$$\mathbf{F}(\mathbf{x}) = 2A \nabla(\Phi^2) + (1 - 2A) 2\Phi \nabla \Phi. \quad (5)$$

Here, A is the free parameter that allows one to tune the coexistence curve in accordance with the equation of state.

III. BOUNDARY CONDITIONS

The calculation are performed in a rectangular domain with dimensions of L_x, L_y, L_z . The periodic boundary condition are used in x and y directions. We use the “bounce-back” rule in the LBM simulations to implement the no-slip boundary conditions at the solid substrate at $z = 0$.

One of the simple models of solid substrate wettability is to introduce interaction forces between a fluid node \mathbf{x} and the nearest five solid nodes (Fig. 2, the red points)

$$\mathbf{F}(\mathbf{x}) = B \Phi(\mathbf{x}) \sum_{k=1}^5 w_k \Phi_{\text{solid}}(\mathbf{x} + \mathbf{e}_k) \cdot \mathbf{e}_k. \quad (6)$$

Here, the values of function Φ_{solid} take the same values as in adjacent nodes of fluid. Hence, we have $\Phi_{\text{solid}}(\mathbf{x} + \mathbf{e}_6) = \Phi(\mathbf{x})$, where \mathbf{e}_6 is the lattice vector directed from a node \mathbf{x} vertically down to solid surface (see Fig. 2).

The parameter B allows one to control the value of wettability (adhesion) of the solid surfaces. For the surface of neutral wettability (wetting angle = 90 degrees), the parameter is $B = 1$. For the superhydrophobic substrate $B \ll 1$.

IV. ELECTRIC FORCES CALCULATIONS

If free electrical charges are absent, the body force acting on a dielectric liquid in an electric field is given by the Helmholtz formula [21]

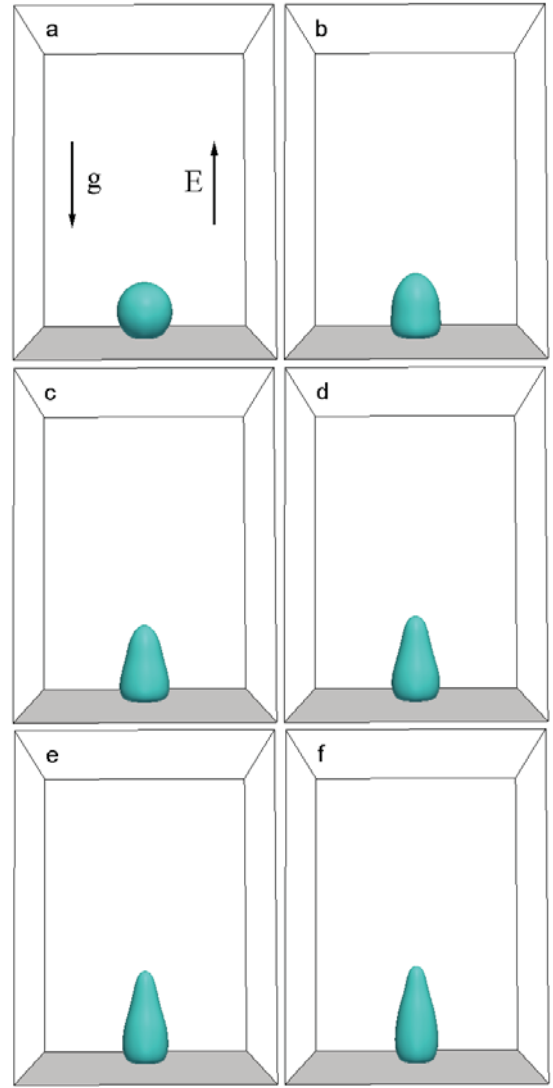


Fig. 3. Initial stage of the droplet evolution. $t = 400$ (a), 1200 (b), 1800 (c), 2200 (d), 2600 (e), 3000 (f). Lattice $400 \times 400 \times 544$ ($\approx 90\,000\,000$ nodes). $\epsilon_l = 4.0$. $R_0 = 50$, $\text{Bo} = 0.26$, $\text{Bo}_e = 17.5$, $\text{Oh} = 0.039$.

$$\mathbf{F} = -\frac{\epsilon_0 E^2}{2} \nabla \epsilon + \frac{\epsilon_0}{2} \nabla \left[E^2 \rho \left(\frac{\partial \epsilon}{\partial \rho} \right)_T \right]. \quad (7)$$

The first term represents the action of an electric field on polarization charges in a nonuniform dielectrics. The second term describes the electrostriction forces. We take into account both terms in our 3D simulations.

The calculations of electric field are carried out taking into account the variation of the permittivity distribution in space and the change of it in time. Hence, we solve the following equation for the distribution of the electric field potential φ between electrodes

$$\text{div}(\epsilon_0 \epsilon \text{grad} \varphi) = 0. \quad (8)$$

The dielectric permittivity of liquid is ϵ_l , and the value of $\epsilon = 1$ is valid for vapor.

The periodic boundary conditions are used along the x and y coordinates. The value of the potential at the upper

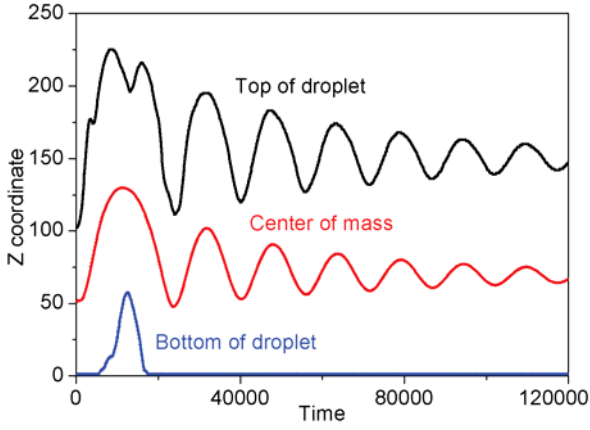


Fig. 4. Time dependences of the top, bottom and center of mass of the droplet. $\epsilon_l = 4.0$. Lattice $400 \times 400 \times 544$. $R_0 = 50$, $Bo = 0.26$, $Bo_e = 17.5$, $Oh = 0.039$.

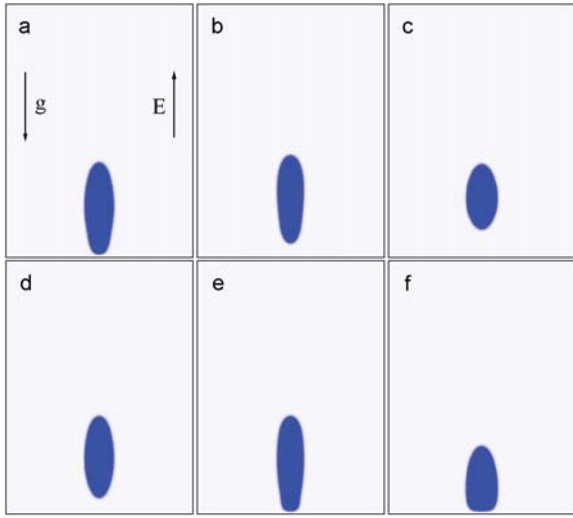


Fig. 5. Jump of the droplet (a-f). $t = 6000$ (a), 10000 (b), 12400 (c), 15000 (d), 17000 (e). Approximately final droplet shape $t = 120000$ (f).

boundary of the calculation domain is $\varphi(x, y, L_z) = -V$. At the solid substrate, we have $\varphi(x, y, 0) = 0$.

We solve the equation (8) for the electric potential at each time step using the well-known method of simple iterations for the potential that can be written in the form

$$\varphi^{n+1}(\mathbf{x}, t) = \frac{\sum_{k=1}^6 (\epsilon(\mathbf{x}, t) + \epsilon(\mathbf{x} + \mathbf{c}_k \Delta t, t)) \varphi^n(\mathbf{x} + \mathbf{c}_k \Delta t)}{\sum_{k=1}^6 (\epsilon(\mathbf{x}, t) + \epsilon(\mathbf{x} + \mathbf{c}_k \Delta t, t))}. \quad (9)$$

The initial values of the potential are taken from the previous time step $\varphi^0(\mathbf{x}, t) = \varphi(\mathbf{x}, t - \Delta t)$. This approach is a very good initial approximation for iterations because the density distribution and, consequently, permittivity distribution $\epsilon(\mathbf{x}, t)$ are not changed noticeably during one time step. The electric field can be calculated as $\mathbf{E} = -\nabla \varphi$.

V. COMPUTER SIMULATIONS

The droplet tends to elongate in the direction of electric field. The degree of elongation increases with the increasing

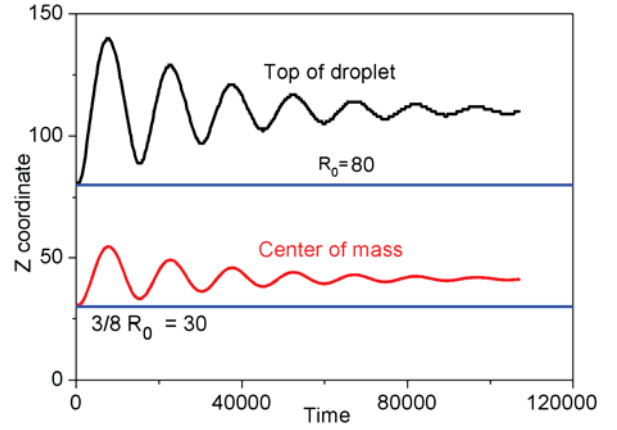


Fig. 6. Time dependences of the droplet top and center of mass. $\epsilon_l = 2.0$. Lattice $400 \times 400 \times 544$. $R_0 = 80$, $Bo = 0.67$, $Bo_e = 14.6$, $Oh = 0.030$.

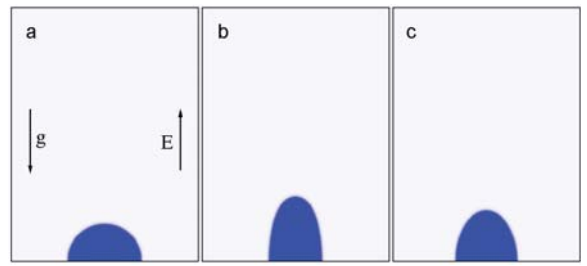


Fig. 7. Initially hemispherical droplet in the electric field. The initial (a) and final (c) shapes of the droplet. $t = 0$ (a), 8000 (b), 107000 (c).

voltage. The initial oscillations decay with time, and the droplet acquires its equilibrium shape. The dimensionless parameters governing the droplet behavior are the gravitational Bond number $Bo = \rho g R_0^2 / \sigma$ and the electrical Bond number $Bo_e = \epsilon_0 (\epsilon_l - 1) E^2 R_0 / \sigma$ (the electrical capillary number), where σ is the surface tension. Hence, the surface tension plays an important role during the process of deformation of droplets.

This process depends also on the kinematic viscosity of liquid ν (the Ohnesorge number $Oh = \nu \sqrt{\rho / (\sigma R_0)}$). The elongation of the droplet in the electric field without gravity is also simulated as the test problem. In this case, the final shape of the droplet is an ellipsoid elongated in the direction of the electric field.

The initial stage of the droplet deformation on superhydrophobic substrate at the electrical Bond number $Bo_e = 17.5$ is shown in Fig. 3. After the application of voltage, the droplet begins to elongate in the direction of electric field. The apex of the droplet begins to move upward. Simultaneously, the center of mass also moves upward (Fig. 4). Further, the center of mass moves by inertia. At the small values of the parameter of adhesion $B = 0.1$, the attractive forces (6) between droplet and substrate (wettability) are small. Hence, at time $t \approx 7000$, the droplet comes off the substrate and jumps over the solid substrate (Figs. 4 and 5). At the same time, the oscillations of the drop shape occur (Figs. 4 and 5). The maximum distance of the droplet from the plane is reached at about $t \approx 12000$

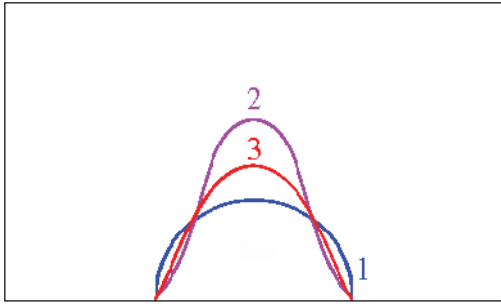


Fig. 8. Hemispherical pinned droplet in the electric field. Curves 1 is the initial shape, curve 2 is the maximum height and curve 3 is the final shape of the droplet. $t = 0$ (1), 5400 (2), 114000 (3). $\mathcal{E}_l = 2.3$. Lattice $400 \times 400 \times 544$. $R_0 = 80$, $Bo = 0.67$, $Bo_e = 18.9$, $Oh = 0.030$.

(Fig. 5,c). Approximately final droplet shape is shown in Fig. 5,f.

The dynamics of a droplet on the wettable surface for the contact angle of 90 degrees is shown in Figs. 6 and 7. In this case, the initial position of the center of mass of the hemispherical droplet is $3/8 R_0$ in accordance with the theoretical value. Then, the droplet begins to elongate in the direction of the electric field. After several oscillation, the droplet acquires its equilibrium shape (Fig. 7,c).

We also simulate a dynamics of the pinned droplet (Fig. 8). In this case, the position of a contact line is fixed and it does not move. After the electric field is applied, the oscillations of initially hemispherical droplet begin. The maximum height of the droplet at the first oscillation is shown in Fig. 8 by curve 2. Simultaneously, the contact angle reduces. The final shape of the droplet is shown in Fig. 8 by the curve 3. The similar results were obtained in [4] for nearly hemispherical conducting drop if zero-field contact angle is equal to 90 degrees. However, the pinned drop was considered in [4] as static.

VI. CONCLUSION

The 3D electrohydrodynamic model of non-stationary dynamics of dielectric droplets on a solid substrate in the surrounding gas is developed. The equations for the potential of electric field and for the fluid dynamics are solved together. The behavior of dielectric droplets on wettable and superhydrophobic surfaces under the action of an electric field is considered. The dynamics of the pinned droplet is also simulated. In all simulations, the droplets begin to elongate in the direction of electric field. Moreover, the droplet on a superhydrophobic solid substrate can jump above the plane after the DC electric field is applied. Thus, the lattice Boltzmann method is a powerful tool for modeling such complex multiphysical phenomena.

REFERENCES

- [1] M. J. Gibbons, C. M. Howe, P. Di Marco, and A. J. Robinson, "Local heat transfer to an evaporating sessile droplet in an electric field," *J. Phys.: Conf. Ser.*, vol. 745, no. 3, p. 032066, 2016.
- [2] Y. Liu, K. Oh, John G. Bai, C.-L. Chang, W. Yeo, J.-H. Chung, K.-H. Lee, and W. K. Liu, "Manipulation of nanoparticles and biomolecules by electric field and surface tension," *Comput. Methods Appl. Mech. Eng.*, vol. 197, no. 25-28, pp. 2156–2172, 2008.
- [3] V. Vancauwenberghe, P. Di Marco, and D. Brutin, "Wetting and evaporation of a sessile drop under an external electrical field: A review," *Colloids and Surfaces A: Physicochem. Eng. Aspects*, vol. 432, pp. 50–56, 2013.
- [4] L. T. Corson, C. Tsakonas, B. R. Duffy, N. J. Mottram, I. C. Sage, C. V. Brown, and S. K. Wilson, "Deformation of a nearly hemispherical conducting drop due to an electric field: Theory and experiment," *Phys. Fluids*, vol. 26, no. 12, p. 122106, 2014.
- [5] L. T. Corson, N. J. Mottram, B. R. Duffy, and S. K. Wilson, "Dynamic response of a thin sessile drop of conductive liquid to an abruptly applied or removed electric field," *Phys. Rev. E*, vol. 94, no. 4, p. 043112, 2016.
- [6] A. Moukengué Imano and A. Beroual, "Deformation of water droplets on solid surface in electric field," *J. Colloid and Interf. Sci.*, vol. 298, no. 2, pp. 869–879, 2006.
- [7] G. Taylor, "Desintegration of water drops in an electric field," *Proc. Royal Soc. London. Ser. A Math. Phys. Sci.*, vol. 280 (1382), pp. 383–397, 1964.
- [8] S. M. Korobeynikov, A. V. Ridel, and D. A. Medvedev, "Deformation of bubbles in transformer oil at the action of alternating electric field," *Europ. J. Mech. B/Fluids*, vol. 75, pp. 105–109, 2019.
- [9] M. Akbari and S. Mortazavi, "Three-dimensional numerical simulation of deformation of a single drop under uniform electric field," *J. Appl. Fluid Mech.*, vol. 10, no. 2, pp. 693–702, 2017.
- [10] Y. Wang, D. Sun, A. Zhang, and B. Yu, "Numerical simulation of bubble dynamics in the gravitational and uniform electric fields," *Numer. Heat Tr. A: Appl.*, vol. 71, no. 10, pp. 1034–1051, 2017.
- [11] G. R. McNamara and G. Zanetti, "Use of the Boltzmann equation to simulate lattice-gas automata," *Phys. Rev. Lett.*, vol. 61, no. 20, pp. 2332–2335, 1988.
- [12] A. L. Kupershtokh and D. A. Medvedev, "Lattice Boltzmann method in hydrodynamics and thermophysics," *J. Phys.: Conf. Ser.*, vol. 1105, p. 012058, 2018.
- [13] A. L. Kupershtokh, "Three-dimensional LBE simulations of a decay of liquid dielectrics with a solute gas into the system of gas-vapor channels under the action of strong electric fields," *Comput. Math. Appl.*, vol. 67, no. 2, pp. 340–349, 2014.
- [14] Y. H. Qian, D. d'Humières, and P. Lallemand, "Lattice BGK models for Navier – Stokes equation," *Europhys. Lett.*, vol. 17, pp. 479–484, 1992.
- [15] J. M. V. A. Koelman, "A simple lattice Boltzmann scheme for Navier–Stokes fluid flow," *Europhys. Lett.*, vol. 15, no. 6, pp. 603–607, 1991.
- [16] A. L. Kupershtokh, "New method of incorporating a body force term into the lattice Boltzmann equation," *Proc. 5th International EHD Workshop, Poitiers, France*, pp. 241–246, 2004.
- [17] A. L. Kupershtokh, "Criterion of numerical instability of liquid state in LBE simulations," *Comput. Math. Appl.*, vol. 59, no. 7, pp. 2236–2245, 2010.
- [18] Y. H. Qian and S. Chen, "Finite size effect in lattice-BGK models," *Int. J. Mod. Phys. C*, vol. 8, no. 4, pp. 763–771, 1997.
- [19] A. L. Kupershtokh, D. I. Karpov, D. A. Medvedev, C. P. Stamatelatos, V. P. Charalambakos, E. C. Pyrgioti, and D. P. Agoris, "Stochastic models of partial discharge activity in solid and liquid dielectrics," *IET Sci. Meas. Technol.*, vol. 1, no. 6, pp. 303–311, 2007.
- [20] A. L. Kupershtokh, D. A. Medvedev, and D. I. Karpov, "On equations of state in a lattice Boltzmann method," *Comput. Math. Appl.*, vol. 58, no. 5, pp. 965–974, 2009.
- [21] L. D. Landau and E. M. Lifshitz, *Electrodynamics of Continuous Media*. Pergamon Press, Oxford, 1959.